Supplemental Figures

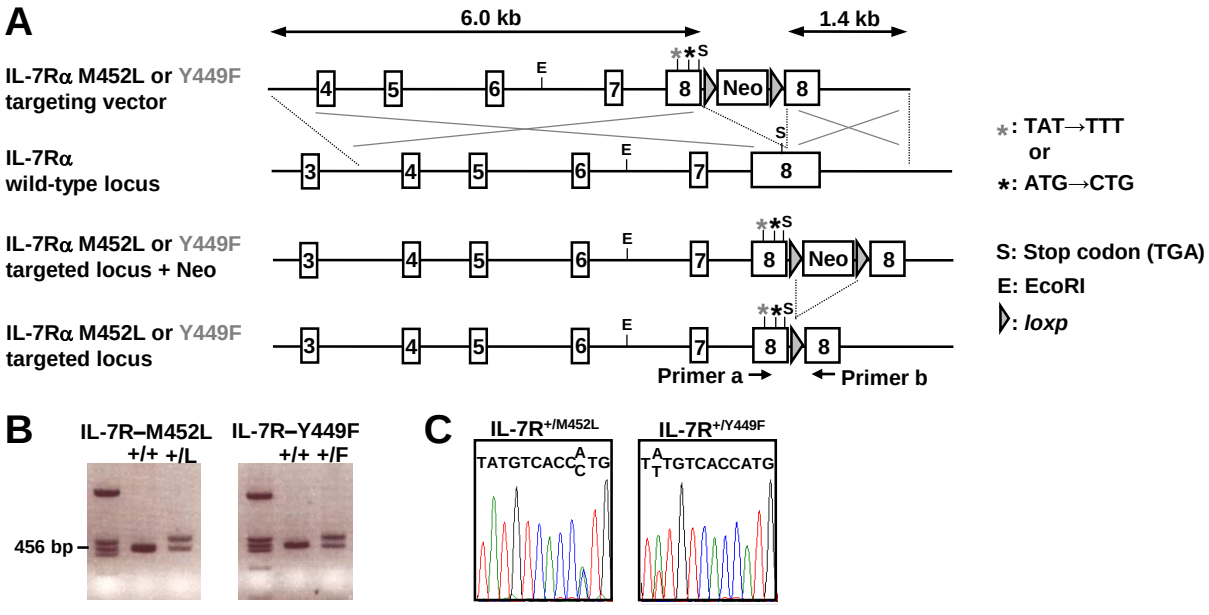

Supplemental Figure 1. Generation of IL-7R–Y449F and IL-7R–M452L mice.

(**A**) Targeting strategy for IL-7R–M452L and IL-7R–Y449F knock-in alleles. Boxes indicate exons. Asterisks show point mutations. Triangles indicate *lox*P sequences. The neomycin (Neo) resistance gene cassette was excised by Cre recombination. (**B**) Genotyping PCR to detect the knock-in alleles by primers a and b, as shown in (A). (**C**) DNA sequencing confirmed point mutations in heterozygous IL-7R–M452L and IL-7R–Y449F mice.

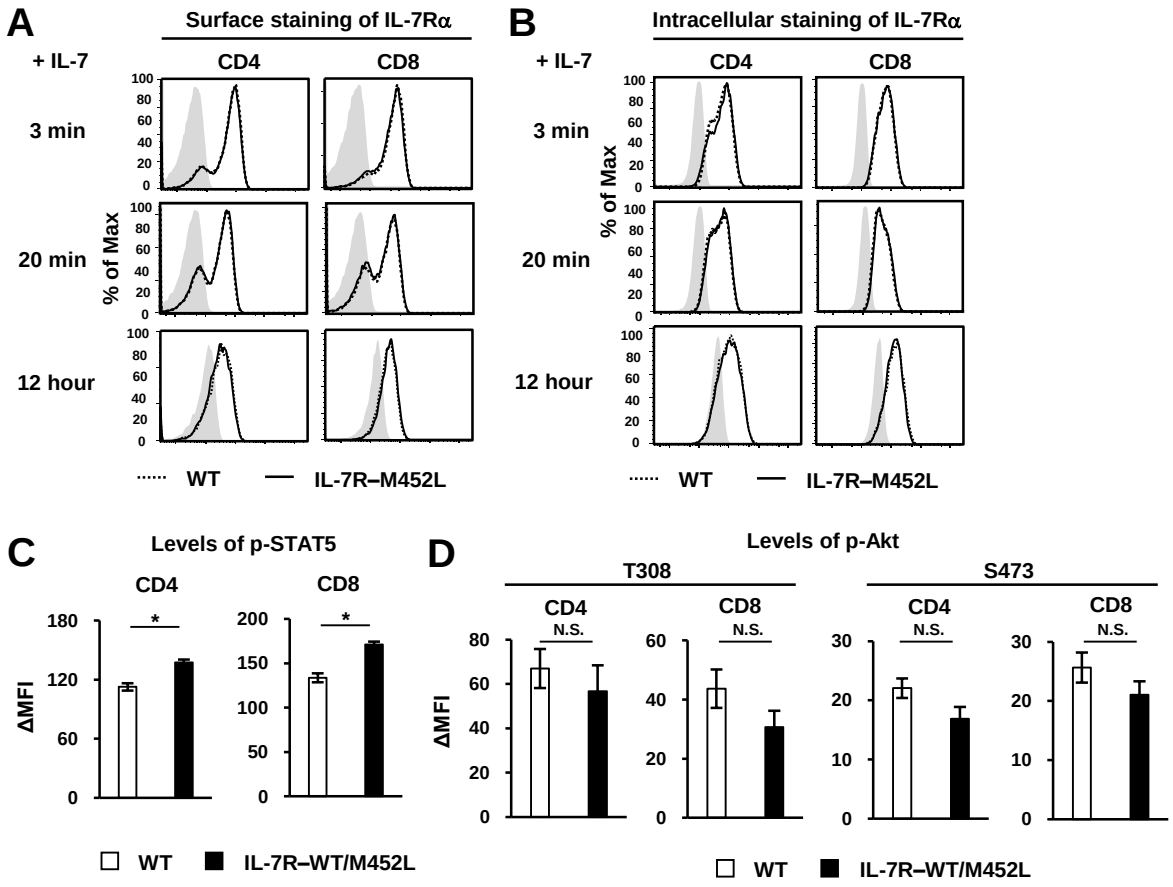

Supplemental Figure 2. IL-7R expression and signal transduction in IL-7R-M452L and IL-7R-WT/M452L heterozygous mice.

(**A**) Flow cytometric analysis of IL-7Rα expression on cell surface of naive CD4 and CD8 T cells from WT or IL-7R–M452L mice at 3 and 20 minutes, or 12 hours after stimulation with 10 ng/ml IL-7. (**B**) Flow cytometric analysis of intracellular staining for IL-7Rα in naive CD4 and CD8 T cells as (A). Gray shaded curves, isotype-matched control antibody. (**C**) The difference in mean fluorescence intensity (ΔMFI) between p-STAT5 and isotype controls in naive T cells from WT and IL-7R–WT/M452L heterozygous mice at 20 minutes after stimulation with 10 ng/ml IL-7 (n = 4). (**D**) The ΔMFI between p-Akt and isotype controls in naive T cells from WT and IL-7R–WT/M452L heterozygous mice at 12 hours after stimulation with 10 ng/ml IL-7 (n = 4). Data represent two to three independent experiments with similar results. Data are means ± SEM with Student's t-test. *, $p < 0.05$; N.S., not significant.

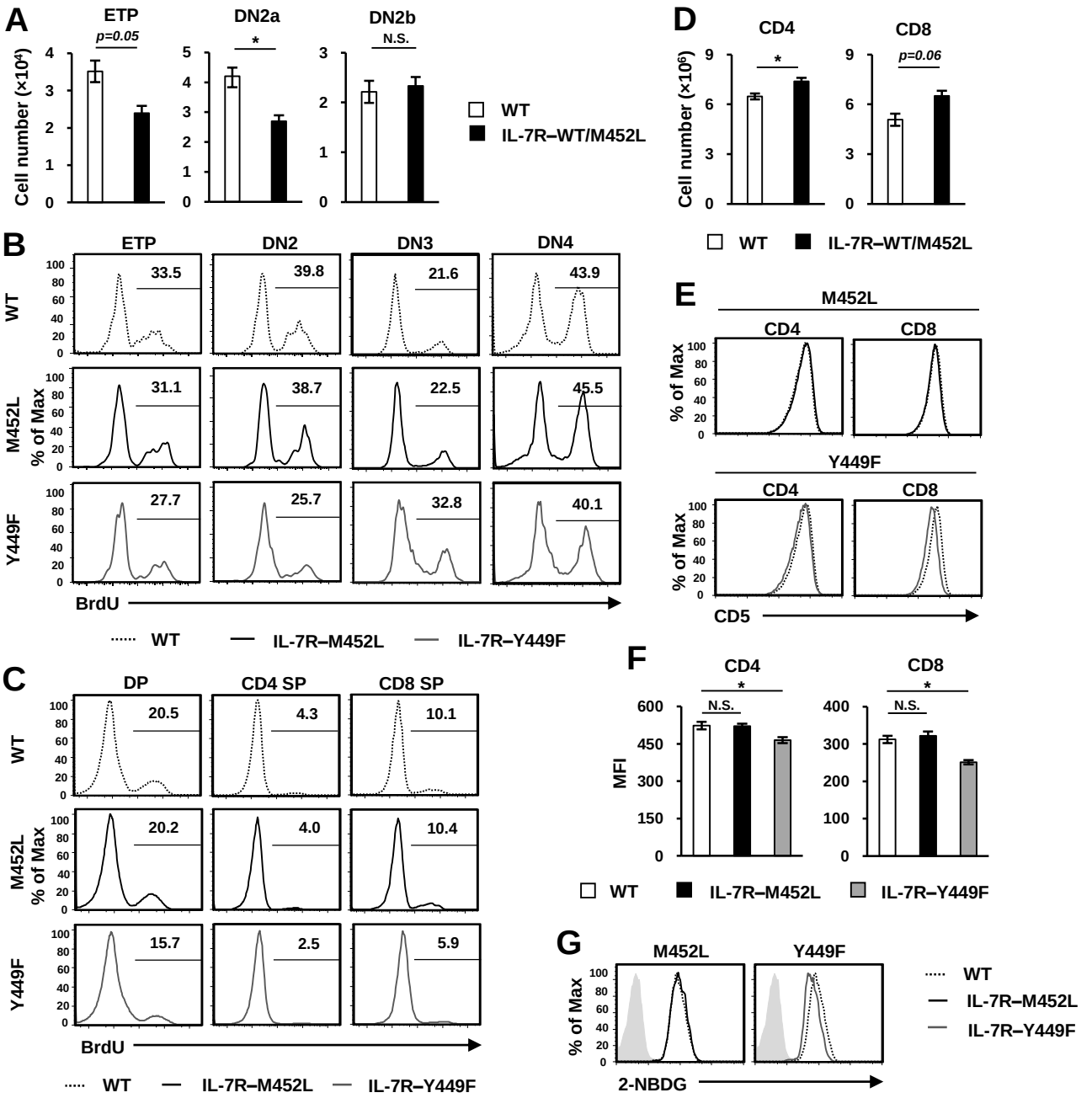

Supplemental Figure 3. Thymocytes and lymph node T cells in IL-7R–Y449F, IL-7R–M452L, or IL-7R-WT/M452L heterozygous mice.

(**A**) Cell numbers of ETP, DN2a and DN2b thymocytes in WT and IL-7R–WT/M452L heterozygous mice (n = 5). (**B**) BrdU uptake by DN thymocytes 9 hours after intraperitoneal (i.p.) injection. (**C**) BrdU uptake by DP and SP thymocytes 12 hours after i.p. injection. (**D**) Cell numbers of lymph node T cells of WT and IL-7R–WT/M452L heterozygous mice (n = 5). (**E**) Flow cytometry analysis for surface expression of CD5 on lymph node T cells of WT, IL-7R–Y449F, and IL-7R–M452L mice. (**F**) Mean fluorescence intensity (MFI) values of CD5 expression, as shown in (E) (n = 4). (**G**) Glucose uptake was assessed in naive CD4 T cells by 2-(N-(7nitrobenz-2-oxa-1,3-diazol-4-yl)amino)-2-deoxyglucose (2-NBDG) (n = 3). Gray shaded curves, glucose control. Data represent two to three independent experiments with similar results. Data are means ± SEM with Student's t-test (A and D) and one-way ANOVA (F). *, $p < 0.05$; N.S., not significant.

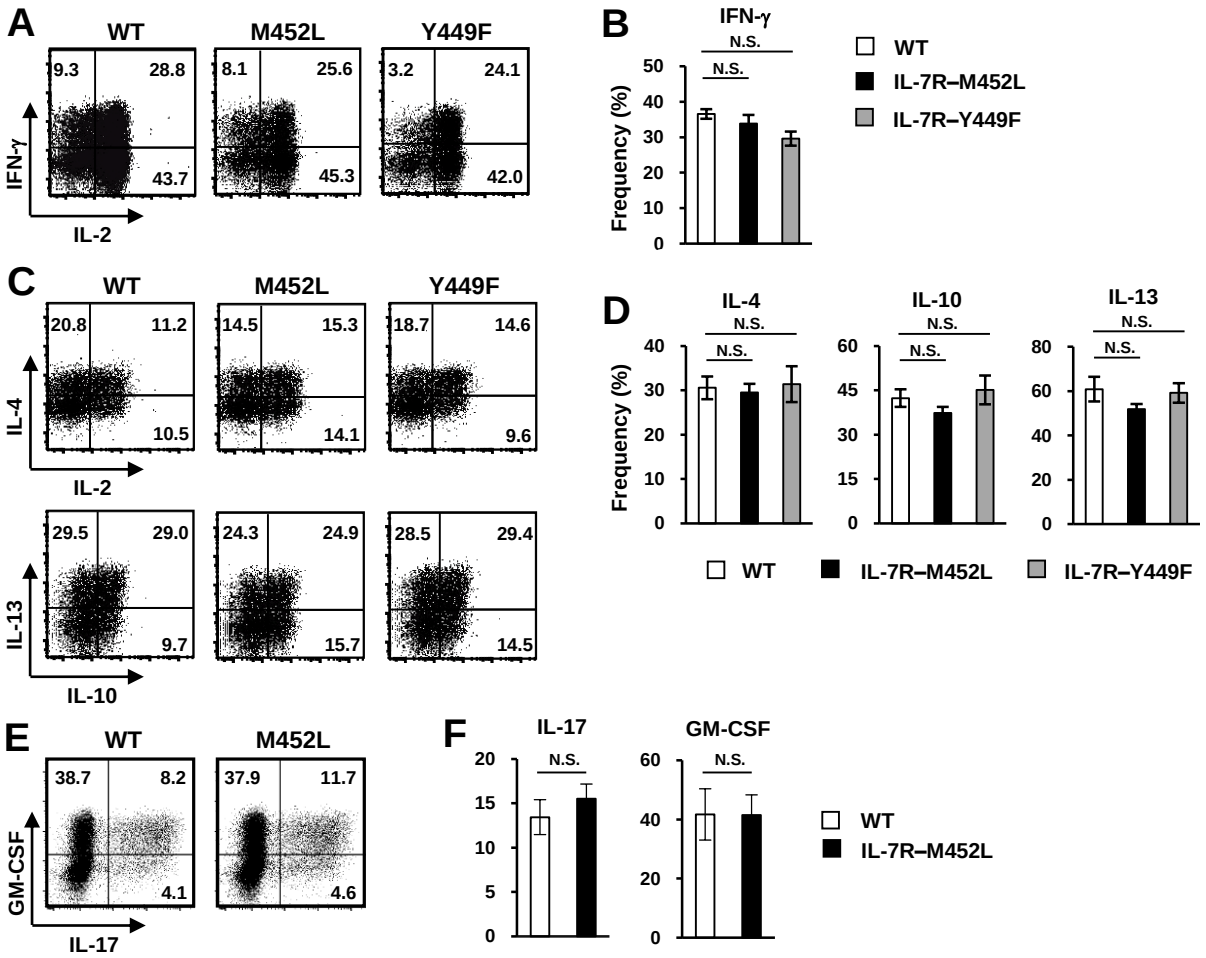

Supplemental Figure 4. Th differentiation in IL-7R–Y449F and IL-7R–M452L T cells.

(**A**) Naive CD4 T cells from lymph nodes of WT, IL-7R–Y449F, and IL-7R–M452L mice were cultured with 20 ng/ml IL-7 under Th1 conditions for 6 days. Intracellular cytokine staining was performed following PMA and ionomycin stimulation for 4 hours. (**B**) Frequency of IFN-γ–producing cells, as shown in (A) (n = 3). (**C**) Naive CD4 T cells were cultured with 20 ng/ml IL-7 under Th2 conditions for 6 days. Intracellular cytokine staining was performed following PMA and ionomycin stimulation for 4 hours. (**D**) Frequency of IL-4–, IL-10–, and IL-13–producing cells, as shown in (C) (n = 3). (**E**) Naive CD4 T cells from lymph nodes of WT and IL-7R–M452L mice were cultured under Th17 conditions without IL-7 for 4 days. Intracellular cytokine staining was performed. (**F**) Frequency of IL-17–producing and GM-CSF–producing cells, as shown in (E) (n = 3). Data represent two independent experiments with similar results. Data are means ± SEM with one-way ANOVA (B and D) and Student's t-test (F). N.S., not significant.